

Photorefractive Effect in a New Composite Based on Bifunctional Host Polymer

YI-WANG CHEN,¹ YUAN-KANG HE,¹ HUI-YING CHEN,¹ FENG WANG,² ZHI-JIAN CHEN,² QI-HUANG GONG²

¹ College of Chemistry, Peking University, Beijing, 100871, People's Republic of China

² Department of Physics, Peking University, Beijing, 100871, People's Republic of China

Received 15 January 1999; accepted 10 October 1999

ABSTRACT: A new photorefractive composite based on a bifunctional methacrylate copolymer with *N*-methacryloxypropyl-3-(*p*-nitrophenyl)azo carbazole and *N*-methacryloxypropyl carbazole as pendant side chains, which has high stability and potential applications, was synthesized. A two-beam coupling gain coefficient of 9.4 cm^{-1} and an electrooptic coefficient of 9.3 pm/V were measured at the applied electric field of $92.4 \text{ V}/\mu\text{m}$ by a typical two-beam coupling experiment and a compensation electrooptic measurement technique. © 2000 John Wiley & Sons, Inc. *J Appl Polym Sci* 77: 189–194, 2000

Key words: side-chain polymer; polymeric modifying; polymeric composite; photorefractive effect; two-beam coupling experiment

INTRODUCTION

The driving force to pursue research on photorefractive (PR) polymers comes from both fundamental interests and practical expectations. It has been known that photorefractive materials are multifunctional materials which combine the electrooptic (EO) effect and photoconductivity to manifest a new property: photorefractivity.¹ Photorefractivity has been demonstrated so far in guest–host systems^{2–5} where a glassy polymer matrix is doped with either a transport agent, a photosensitizer, an electrooptical molecule (NLO chromophores), or sometimes a plasticizer. The electrooptic effect due to alignment of the chromophores is achieved by applying a field to the sandwiched polymer or by corona poling. The guest–host approach most probably leads to a polymeric system with low stability. On the other hand, photorefractivity was observed in some side-chain polymeric materials^{6–8} which have both the photoconductivity and the electrooptic

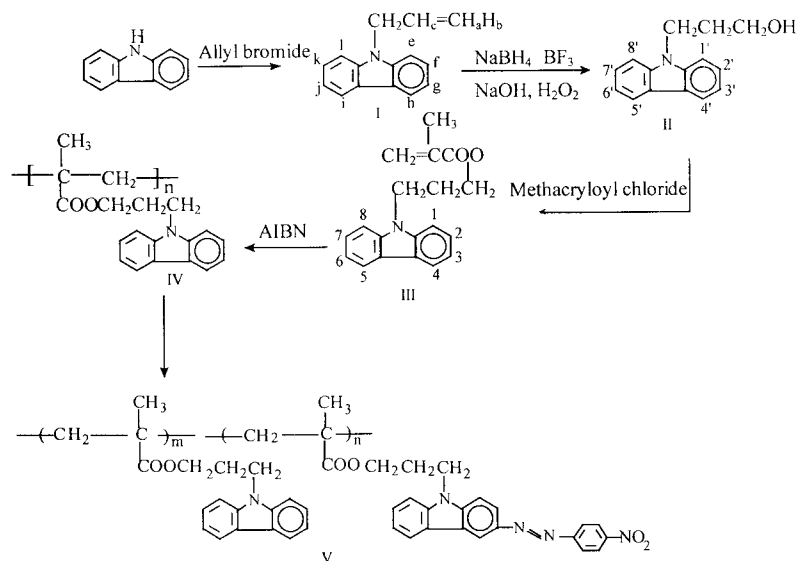
effect intrinsically. To obtain a photorefractive composite based on a side-chain host polymer, modified polyvinylcarbazole (PVK) was used as starting material since it is well known for its photoconductive properties.^{9–12} We synthesized a new side-chain polymeric material with poly(carbazolylpropyl methacrylate) (PCPMA) as a starting reagent. A portion of the carbazole groups were reacted with *p*-nitrophenylazonium to form 3-(*p*-nitrophenyl)azo carbazole (NPAC) groups with second-order NLO properties. The nonlinear chromophores, in this case, are attached to the backbone as a side chain and higher stability of the EO effect is obtained. In this article, we also report the observation of photorefractivity in a carbazole-(nitrophenyl)azo carbazole (PCPMA–NPAC) polymeric system. Two-beam coupling (2BC) and EO experiments were performed, and the 2BC gain coefficient and EO coefficient were measured as a function of the applied electric field. The erase–write properties of the gratings are discussed as well.

EXPERIMENTAL

The synthetic procedures and the chemical structure of PCPMA–NPAC are shown in Scheme 1.

Correspondence to: H. Y. Chen (hychen@chemms.chem.pku.edu.cn).

Journal of Applied Polymer Science, Vol. 77, 189–194 (2000)
© 2000 John Wiley & Sons, Inc.



Scheme 1 Synthesis and chemical structure of side-chain polymer PCPMA-NPAC ($m : n = 0.8 : 0.2$).

Preparation of 9-Allylcarbazole (I)

To a mixture of 6.68 g (0.04 mol) carbazole, 35 mL aqueous 50% sodium hydroxide, 5 mL benzene, and 410 mg (1.8 mmol) benzyltriethylammonium chloride, 5.19 mL (0.06 mol) of allylbromide was added dropwise with stirring. It was continued at room temperature for 2 h. Then, the reaction mixture was poured into hot water and left overnight at room temperature. The precipitated solid was collected, washed with water, and dried. Recrystallizations from ethanol afforded colorless plates (mp 52–54°C).

$^1\text{H-NMR}$ (400 MHz, CDCl_3): δ (ppm) = 4.905 (2H, d, CH_2), 5.140 (1H, d, CH_a), the foot number set the structural formula of Scheme 1), 5.167 (1H, d, CH_b), 5.910 (1H, m, CH_c), 7.244 (2H, d, H_e, H_1), 7.368 (2H, t, H_g, H_j), 7.438 (2H, t, H_f, H_k), 8.102 (2H, d, H_h, H_i).

Preparation of 9-(3-Hydroxypropyl)carbazole (II)

In a 300-mL flask, fitted with a dropping funnel, a reflux condenser, a nitrogen inlet tube, and a magnetically operated stirring bar, was placed 41 mL of a 1.00M solution (1.55 g sodium borohydride in THF) and 10.35 g 9-allylcarbazole (50 mmol) in 50 mL THF. The flask was immersed in an ice-water bath at 0°C and flushed with dry nitrogen. A static nitrogen atmosphere was then maintained. From the dropping funnel, 10.5 mL of borontrifluoride etherate (82 mmol) was added dropwise to the reaction mixture over a period of 30 min. The flask was kept for 1 h at 20–25°C.

Excess hydride was destroyed by the careful addition of 20 mL of water. The organoborane was oxidized at 30–50°C by adding 6 mL of 3 N NaOH followed by the dropwise addition of 6 mL of 30% H_2O_2 . The warm reaction mixture was stirred for an additional hour at room temperature. After the addition of 50 mL water, THF was evaporated out and the product was extracted with ether. Finally, the product was recrystallized from methanol twice (mp 96–98°C).

$^1\text{H-NMR}$ (400 MHz, CDCl_3): δ (ppm) = 1.537 (1H, s, OH), 2.085 (2H, quartet, CCH_2C), 3.574 (2H, t, NCH_2), 4.439 (2H, t, OCH_2), 7.221 (2H, d, 1', 8'-H), 7.449 (4H, t, 2', 3', 6', 7'-H), 8.090 (2H, d, 4', 5'-H).

Preparation of 3-(N-Carbazolyl)propyl Methacrylate (III)

In a dry 250-mL three-necked flask, 2.9 mL of methacryloyl chloride in 20 mL of dry dichloromethane was added to a solution of 5.6 g 9-(3-hydroxypropyl)carbazole and 4.2 mL of triethylamine in 80 mL of dichloromethane. After stirring for 3 h, the reaction mixture was washed with 2 N NaOH and water. The crude product was further purified by column chromatography with dichloromethane as an eluent. Yield: 5.11 g (70%) of a colorless oil.

ANAL. Calcd (found): C, 77.81% (77.87%); H, 6.48% (6.47%); N, 4.78% (4.73%).

$^1\text{H-NMR}$ (400 MHz, CDCl_3): δ (ppm) = 1.975 (3H, s,

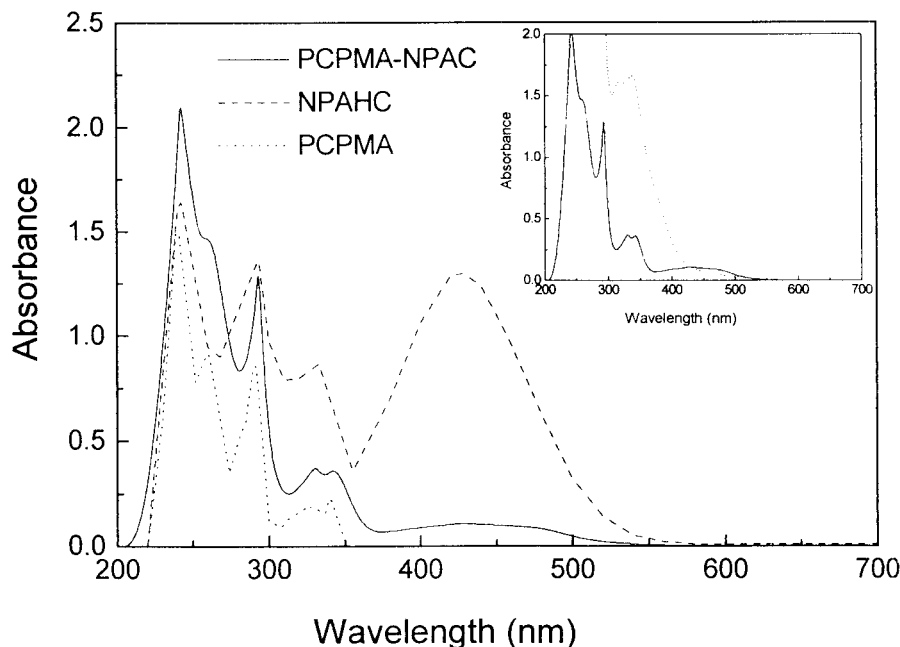


Figure 1 UV/vis spectra of (solid line) PCPMA–NPAC, (dotted line) PCPMA, and (dashed line) NPAHC. Insert: (solid line) PCPMA–NPAC; (dotted line) TNF : PCPMA–NPAC.

CH₃), 2.236 (2H, m, CCH₂C), 4.143 (2H, t, NCH₂), 4.413 (2H, t, OCH₂), 5.603 (1H, s, =CH), 6.130 (1H, s, =CH), 7.225 (2H, d, 1, 8-H), 7.366 (2H, t, 3, 6-H), 7.426 (2H, t, 2, 7-H), 8.078 (2H, d, 4, 5-H).

Polymerization of Poly[3(*N*-carbazolyl)propyl methacrylate] (PCPMA) (IV)

Polymerization was carried out in purified toluene in a vacuum sealing tube with AIBN as the initiator. The polymer was precipitated out in methanol and purified by redissolving in chloroform and reprecipitation in methanol.

ANAL. Calcd (found): C, 77.81% (76.29%); H, 6.48% (6.53%); N, 4.78% (5.11%).

GPC measurement in THF indicated a weight-average molecular weight of 1.43×10^5 using polystyrene as a standard. DSC and TGA studies showed a glass transition temperature (T_g) of 92°C and a decomposition temperature (T_d) of 437°C.

Synthesis of PCPMA–NPAC (V)

The solution of *p*-nitrophenylazonium chloride produced from 0.34 g of *p*-nitroaniline (2.5 mmol) and 2.5 mmol of HNO₂ in 30 mL water was added to the mixture of 0.73 g of PCPMA (2.5 mmol) and

0.021 g of C₁₂H₂₅C₆H₄SO₃Na in 50 mL dichloromethane in an ice-water bath. After stirring 24 h at this temperature, the products were precipitated from ethanol and purified by redissolving in chloroform and reprecipitation in methanol.

ANAL. (found): C, 75.11%; H, 6.02%; N, 5.54%; O, 12.65%, so the mol ratio of PCPMA to NPAC is 80 to 20. The polymers are red powder and are soluble in a variety of solvents.

UV/vis Spectra

The UV/Vis spectra (Fig. 1) of the polymers and 3(*p*-nitrophenyl)azo-*N*-hydroxyethyl carbazole (NPAHC) (synthesized for comparison) showed the typical absorption at 425 nm of the both NPAHC and NPAC groups, indicating that the NPAC group was already attached on the polymer and the typical absorption wavelength of the charge-transporting compound, namely, the carbazolyl group, at 342 nm. It should be noted that the UV/vis spectra of the mixture of PCPMA–NPAC and 2,4,7-trinitrofluorenone (TNF) (showed in the insert of Fig. 1) indicated that there were charge-transfer complexes formed between the charge-transporting compound and the TNF species.

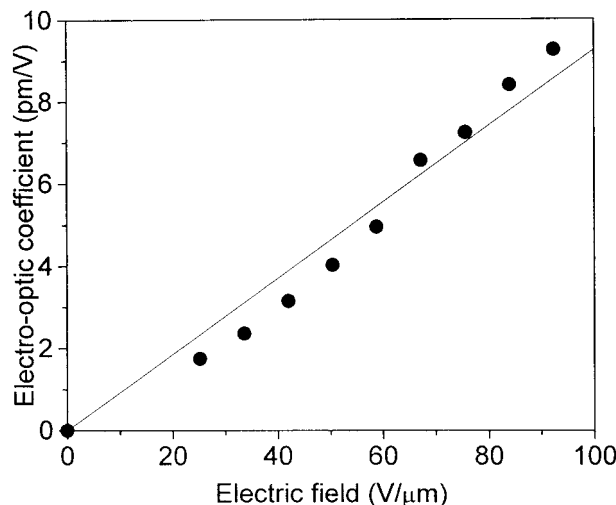


Figure 2 Electric-field dependence of the effective EO coefficient measured at the wavelengths of 632.8 nm.

Poling

To pole the thick samples (100 μm) *in situ* at room temperature to obtain the large birefringence, we modified the polymeric system to obtain a low glass transition temperature (T_g) by adding a plasticizer (9-ethyl carbazole) up to 29 wt %. The composite contained mainly PCPMA–NPAC at a weight ratio of 70%, in which carbazole groups act as photoconductive moieties and NPAC groups provide the NLO property. TNF (1 wt %) was added as the photosensitizer. The sample was sandwiched by two ITO-coated glass slides and a Teflon film was used as a spacer to control the thickness of the sample film. The T_g of the composite was 36°C measured by a differential scanning calorimeter (DSC) and, thus, poling can be carried out by applying a dc electric field directly at room temperature. To detect the photorefractive properties of our low T_g thick samples, electrooptic measurements and two-beam coupling experiments were performed.

RESULTS AND DISCUSSION

Electrooptic (EO) properties of the composite were measured using a compensation EO modulation technique.¹³ A linear polarized 632.8 nm He–Ne laser beam (power 0.2 mW) with a polarization angle of 45° with respect to the plane of incidence was propagated through the sample film at an incident angle of 60° in air and then a parallelly mounted KD*P crystal was used. A dc

voltage was applied to the sample film through the two ITO electrodes. The transmitted beam then passed through an analyzer, whose polarization direction was oriented at 90° with respect to the initial polarization of the incident beam. The phase-difference $\Delta\Phi$ of the *p*- and *s*-polarized components of the beam from both voltage-induced anisotropy and the EO effect of the sample was compensated by using another variable dc voltage on the KD*P crystal. With the measured value of $\Delta\Phi$, we may deduce the effective EO coefficient γ_{eff} through

$$\Delta\Phi = (\pi n_0^3 \gamma_{\text{eff}} V \sin^2 \theta) / \lambda \cos \theta \quad (1)$$

where λ is the wavelength of the laser beam; θ , the incident angle inside of the sample; V , the dc voltage applied on the sample; and n_0 , the refractive index of the polymeric composite film. The value of γ_{eff} was calculated with eq. (1) for the photorefractive sample at a certain dc poling voltage. Figure 2 shows the dependence of the effective EO coefficient on the applied electric field, and a linear relationship is seen. At the applied electric field of 92.4 V/ μm , the γ_{eff} reached 9.3 pm/V.

The photorefractive property of this side-chain polymeric system was verified by using two-beam coupling (2BC) studies at a wavelength of 633 nm. In the 2BC experiments, a typical tilted geometry¹³ was employed as given in Figure 3. Two mutually coherent *p*-polarized He–Ne laser beams with powers of 40 and 30 μW at 633 nm were incident upon the sample. The tilt angle was $\phi_{\text{ext}} = 60^\circ$ and the angle between two beams was $2\theta_{\text{ext}} = 20^\circ$ in air. The characteristic feature of a photorefractive effect is that refractive index

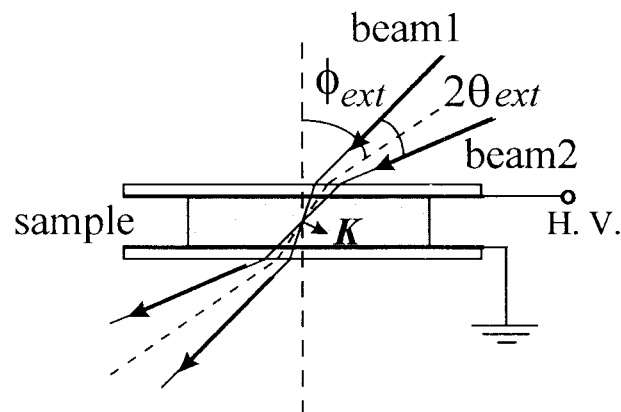


Figure 3 Schematic of the tilted geometry of the two-beam coupling experiment.

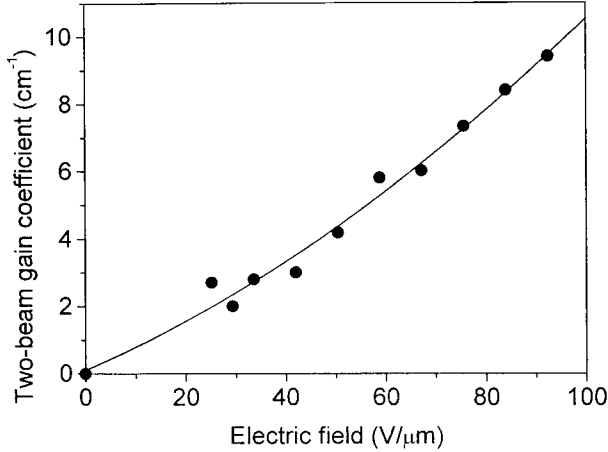


Figure 4 Electric-field dependence of the steady-state 2BC gain coefficient at the wavelength of 632.8 nm.

grating created in the medium shifted spatially with respect to the writing intensity pattern (called a nonlocal response). As a result, an asymmetric energy transfer between write beams in a photorefractive sample occurs. In this experiment, we measured the following physical quantities: I_1 , I_{12} , I_2 , and I_{21} , where I_1 (I_2) and I_{12} (I_{21}) are the intensity of beam 1 (beam 2) after the sample in the absence and in the presence of beam 2 (beam 1), respectively. When the angle between two beams is small enough, the two-beam coupling gain coefficient, Γ , can be calculated by the following approximate formula:¹⁴

$$\Gamma = \frac{\cos \phi}{d} \ln\left(\frac{br}{b+1-r}\right) \quad (2)$$

where $b = I_2/I_1$, $r = I_{12}/I_{21}$, ϕ is the tilting angle inside the sample, and d is the thickness of the sample. The electric-field dependence of the two-beam coupling gain coefficient is presented in Figure 4; the 2BC coefficient of 9.4/cm was obtained at the applied electric field of 92.4 V/ μ m. Considering the EO response in low T_g composites, including both the Pockels effect and the orientational birefringence effect, the electric-field dependence of the grating amplitude Δn can be regarded as¹⁵

$$\Delta n \propto E_0 E_{sc} \quad (3)$$

where E_0 is the applied external electric field, and E_{sc} , the internal space-charge field. According to the standard band-transport model,¹ we fitted the measured 2BC coefficients with function of

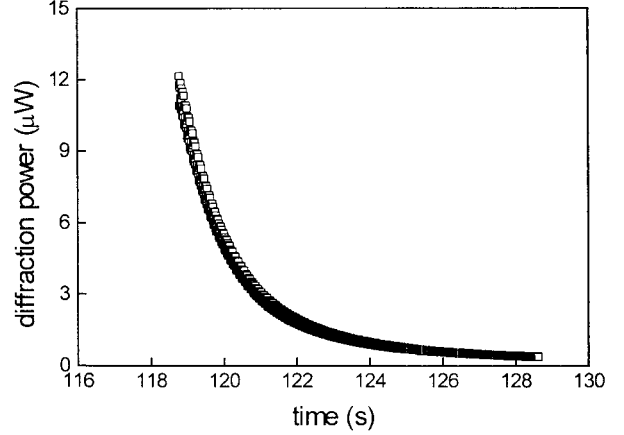


Figure 5 Typical decay trace of the grating erasure.

$$\Gamma = K \frac{E_0 E_0^G}{\sqrt{1 + (E_0^G/E_q)^2}} \sin[\tan^{-1}(E_0^G/E_q)] \quad (4)$$

where E_0^G is the component of E_0 along the direction of the grating wave vector, and E_q , the trapped saturation space-charge field.

The index grating response was also investigated based on the two-beam coupling experiments. After beam coupling reached an equilibrium and, thus, a steady-state grating was created, one of the writing beams was blocked and the other “writing” beam served as both the read-out and erasing beam, and the decay of the PR grating could be recorded. Figure 5 presents the typical process of the grating decay, which followed $\Delta n \propto I^{1/2} = A \exp(-t/\tau)$, where τ is the response time, and I , the intensity. This experiment was repeated with different applied electric

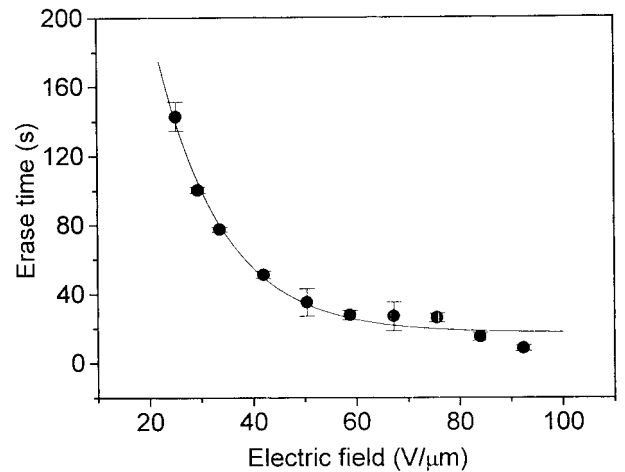


Figure 6 Dependence of the response time on the external electric field at the wavelength of 632.8 nm.

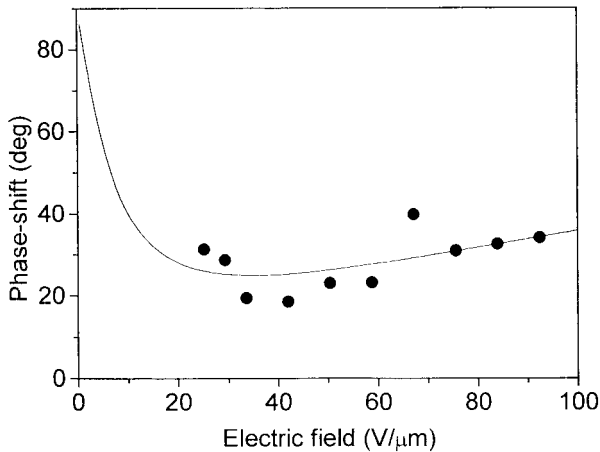


Figure 7 Phase shift as a function of applied field at the four wavelengths of 632.8 nm.

fields at the writing intensity of 0.3 mW/cm^2 . Figure 6 shows the time response characteristic of the PR holograting as a function of the applied field, which can be fitted using an exponential form of $\tau_0 \exp(-E_0/E_m)$, with E_m a parameter dependent on a special sample.¹⁶

By using the fast translation technique,¹⁷ also based on the two-beam coupling experiment, the phase shifts as a function of the applied field were measured and are shown in Figure 7. The experimental data were also fitted theoretically. Different from the processing of 2BC coefficients, we did not neglect the diffusion field E_d here, because we wanted to obtain it from this fit. The fit function is of the form

$$\Psi = \arctan\left(\frac{E_d^2 + E_d E_q + E_0^2}{E_0 E_q}\right) \quad (5)$$

where Ψ is the phase-shift angle. Results suggested that $E_q = 82.9 \text{ V}/\mu\text{m}$ and $E_d = 3.7 \text{ V}/\mu\text{m}$.

CONCLUSIONS

In summary, we have demonstrated a new method to prepare novel photorefractive polymer systems by utilizing the principles for the design of the NLO chromophore. An obvious asymmetric

optical energy exchange was observed, indicating the photorefractive nature of the polymer. Our results indicate that functionalizing a polymeric photoconductor by attachment of second-order moieties as side chains without altering the photogeneration and transport properties of carriers in these amorphous materials is a challenging task. A better understanding of the microscopic mechanisms in this new class of materials has also to be established in order to further improve and optimize their PR performance.

REFERENCES

- Gunter, P.; Huiguand, J. P. *Photorefractive Materials and Their Applications*, Springer-Verlag, Berlin, 1988; Vols. 1 and 2.
- Ducharme, S.; Scott, J. C.; Twieg, R. J.; Moerner, W. E. *Phys Rev Lett* 1991, 66, 1846.
- Silence, S. M.; Walsh, C. A.; Scott, J. C.; Matray, T. J.; Twieg, R. J.; Hache, F.; Bjorklund, G. C.; Moerner, W. E. *Opt Lett* 1992, 17, 1107.
- Cui, Y.; Zhang, Y.; Prasad, P. N.; Schildkraut, J. S.; Williams, D. J. *Appl Phys Lett* 1992, 61, 2132.
- Zhang, Y.; Cui, Y.; Prasad, P. N. *Phys Rev B* 1992, 46, 9900.
- Kippelen, B.; Tamura, K.; Peyghambarian, N.; Padias, A. B.; Hall, H. K., Jr. *Phys Rev B* 1993, 48, 10710.
- Sansone, M. J.; Teng, C. C.; East, A. J.; Kwiatek, M. S. *Opt Lett* 1993, 18, 1400.
- Wang, F.; Chen, Z.; Gong, Q.; Chen, Y.; Chen, H. *Solid State Commun* 1998, 108, 295.
- Stolka, M. In *Encyclopedia of Polymer Science and Engineering*; Wiley: New York, 1998; Vol. 11, p 154.
- Gill, W. D. *J Appl Phys* 1972, 43, 5033.
- Mort, J. *Adv Phys* 1972, 29, 367.
- Borsenberger, P. M.; Ateya, A. I. *J Appl Phys* 1978, 49, 4035.
- Wang, S.; Huang, Z.; Chen, Z.; Gong, Q.; Zhang, Z.; Chen, H. *Chin Phys Lett* 1997, 14, 474.
- Huignard, J. P.; Marrakchi, A. *Opt Commun* 1991, 38, 249.
- Moerner, W. E.; Silence, S. M.; Hache, F.; Bjorklund, G. C. *J Opt Soc Am B* 1994, 11, 320.
- Grunet-Jepsen, A.; Thompson, C. L.; Moerner, W. E. *Appl Phys Lett* 1997, 70, 1515.
- Sutter, K.; Gunter, P. *J Opt Soc Am B* 1990, 7, 2274.